Eur. Phys. J. Special Topics **191**, 147–158 (2010)

DOI: 10.1140/epjst/e2010-01347-3

THE EUROPEAN PHYSICAL JOURNAL SPECIAL TOPICS

Regular Article

Filament capping and nucleation in actin-based motility

M. Faber[1,a], M. Enculescu[2], and M. Falcke[1]

[1] Mathematical Cell Physiology, Max Delbrück Center for Molecular Medicine, Robert Rössle Str. 10, 13092 Berlin, Germany
[2] Institute for Theoretical Physics, Technische Universität, Hardenbergstraße 36, 10623 Berlin, Germany

Received 22 November 2010 / Received in final form 23 December 2010
Published online 18 February 2011

Abstract. Propulsion by actin polymerization is versatilely used in cell motility. Here, we investigate a model of the semi-flexible region of an actin gel close to a propelled object describing the force generation, the dynamics of the propagation velocity, filament attachment to and detachment from the obstacle surface and dynamics of the number of filaments, which result from filament nucleation and capping. The model equations are derived as moment equations of the length distributions. We find a variety of dynamic regimes. The filament number may respond very sensitively to small changes of the attachment rate.

1 Introduction

Force generation by semi-flexible polymers – in particular the cellular polymer actin – is versatilely used for cell motility. The leading edge of lamellipodia of crawling cells [1,4] is pushed forward by a polymerizing actin network and bacteria move inside cells by riding on a comet tail of growing actin filaments [13,23]. The in vivo systems are complemented by in vitro assays using plastic beads and lipid vesicles that, when coated with either ActA or WASP proteins, move much the same way as the pathogens [17,19,22]. The defining feature of semi-flexible polymers is the order of magnitude of their bending energy, which is in the range of $k_{\mathrm{B}}\mathrm{T}$. Consequently they undergo thermal shape fluctuations and the force exerted by the filaments against an obstacle arises from elastic *and entropic* contributions [12,20].

Actin forms a dense network inside lamellipodia of crawling cells. The actin network is stabilized by proteins that cross-link actin filaments. Typical cross-linkers are motor molecules like myosin. They also contract the cytoskeleton and retract the cell body by sliding along the polar filaments. Two regions of the actin network in the lamellipodium can be distinguished. The bulk consists of long cross-linked filaments [26] and is attached to the substrate by integrins. Since this dense actin network has visco-elastic properties and can be described in a continuum approximation [30], we will call this part actomyosin gel. At the leading edge we find the polymerizing

[a] e-mail: Michael.Faber@mpikg.mpg.de

tips of the filaments. The tips are not cross-linked yet [26]. We call this range between leading edge membrane and the average positions of the first cross-linkers semi-flexible region (SR) (see Fig. 1). The SR width of about 0.1 μm is small compared to the gel width of typically 10 μm.

The SR exhibits rich spatio-temporal dynamics. Localized retractions and protrusions of the leading edge travelling along it have been measured indicating an excitable SR dynamics [6,18,25,28]. Spatially modulated oscillatory protrusions and retractions occur as well [6,18]. A recently developed model for the SR exhibits all these dynamic regimes [8,9,11]. However, it did not include dynamics for the density of filaments in the SR. We supplement the model by these dynamics here.

Nucleation of new filaments and capping of the tip of existing ones determine the number of filaments in the SR. Filaments are nucleated in the semi-flexible region close to the leading edge [5,24]. They branch off existing ones, to which they are bound by actin-related protein 2/3 complex (Arp2/3). Branching involves the activation of Arp2/3 by membrane bound Wiskott Aldrich Syndrome protein (WASP) [5,24]. Polymerization is terminated by binding of capping proteins to the filament tips [5,24]. Capped filaments disappear from the SR when the gel boundary moves over their tip position.

2 The model

2.1 Dynamics of length distributions

The length distribution dynamics are determined by the partial differential equations

$$\frac{\partial}{\partial t}N_d(l,t) = \frac{\partial}{\partial l}((\tilde{v}_g - v_p)N_d(l,t)) + k_d N_a(l,t) - k_a N_d(l,t) - k_c N_d(l,t), \tag{1a}$$

$$\frac{\partial}{\partial t}N_a(l,t) = \frac{\partial}{\partial l}(\tilde{v}_g N_a(l,t)) - k_d N_a(l,t) + k_a N_d(l,t) + k_n N_a(l,t), \tag{1b}$$

$$\frac{\partial}{\partial t}N_c(l,t) = \frac{\partial}{\partial l}(\tilde{v}_g N_c(l,t)) + k_c N_d(l,t). \tag{1c}$$

We consider the number densities of three different filament populations: Filaments are attached to the membrane (N_a) by some protein complex, or detached and polymerizing (N_d), or detached and capped (N_c). The actin gel provides support for the filaments in the semi-flexible region, such that they can transfer mechanical momentum to the membrane. The distance between the gel boundary and the membrane is denoted by ζ. We formulate the equations for filaments directed normal to the membrane, since a tilt angle in the experimentally observed range does not cause qualitative changes [8].

The freely fluctuating part of a filament measured from the gel boundary to the tip is flexed by Brownian motion and can be characterized by its contour length l. If the filament is not attached to the membrane, it pushes the membrane with an entropic force F_d. The probability density distribution $P(z)$ of the filament end-to-end distance defines a free energy $\mathcal{F}(z) = -k_B T \ln P(z)$, from which the average normal force on the membrane can be derived as

$$\langle F\rangle(z) = -\frac{\partial \mathcal{F}(z)}{\partial z} = F_c \tilde{F}(\tilde{\eta}).$$

The scale of this force is given by the Euler buckling force

$$F_c = k_B T l_p / l_d^2,$$

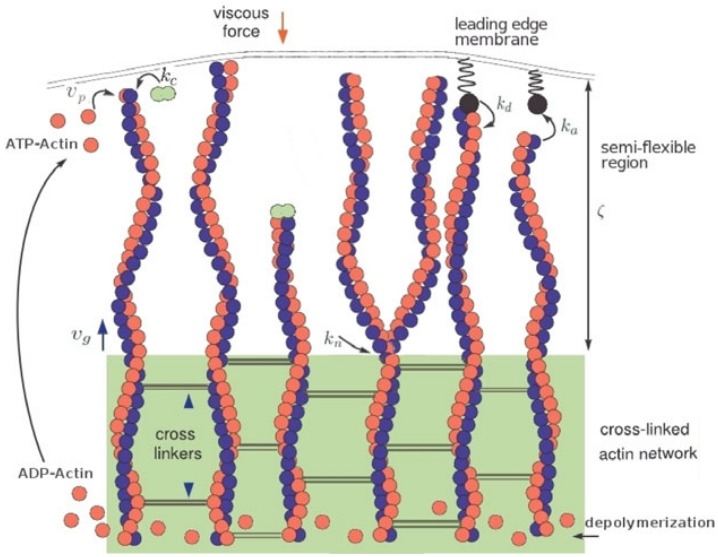

Fig. 1. Processes underlying the model. Close to the leading edge membrane is the semi-flexible region. Cross-linking causes gel formation further away from the membrane. The gel boundary advances with the velocity v_g. Filaments polymerize with the force dependent rate v_p. Polymerization stops when filaments either attach to the membrane with the constant rate k_a or are capped with the force dependent rate k_c. Capped filament tips are left behind when the leading edge and the gel move forward. Attachment is mediated by linker proteins. Attached filaments can either push or pull the membrane. They detach with the force dependent rate k_d. Detached filaments can only push the membrane forward. New filaments are nucleated with rate k_n (see text for details).

where l_p denotes the persistence length of the filament [12,20], and the scaling parameter is given by $\tilde{\eta} = \frac{l_p(l_d-\zeta)}{l_d^2}$. In the following, we use the force dependence on contour length and semi-flexible region depth $F_d(l_d, z)$ in the weakly bending rod approximation derived in [12]. The derivation shows that for small compression $\tilde{\eta} \leq 0.2$ the scaled force reads

$$\tilde{F} = \frac{4e^{-\frac{1}{4\tilde{\eta}}}}{\pi^{\frac{5}{2}}\tilde{\eta}^{\frac{3}{2}}\left[1 - 2\mathrm{erfc}\left(\frac{1}{2\sqrt{\tilde{\eta}}}\right)\right]},$$

and for strong compression

$$\tilde{F} = \frac{1 - 3e^{-2\pi^2\tilde{\eta}}}{1 - \frac{1}{3}e^{-2\pi^2\tilde{\eta}}}.$$

While detached filaments always push the membrane, filaments can, depending on their length, also exert a pulling force during attachment. The molecular details of filament - membrane links are not yet fully known. We therefore assume that single filaments can transiently attach to the membrane with a constant rate k_a via linker proteins, which behave like elastic springs. We distinguish three regimes for the force F_a exerted by the serial arrangement of polymer and linker, depending on the relation between the depth of the semi-flexible region ζ, the equilibrium end-to-end distance

of the filament $R_\parallel$, and the contour length l_a [11]:

$$F_a(l_a, z) = \begin{cases} -k_\parallel(\zeta - R_\parallel),\ \zeta \leq R_\parallel, & \text{i)} \\ -k_{eff}(\zeta - R_\parallel),\ R_\parallel < \zeta < l_a, & \text{ii)} \\ -k_l(\zeta - l_a) - k_{eff}(l_a - R_\parallel),\ \zeta \geq l_a. & \text{iii)} \end{cases} \tag{2}$$

The three cases correspond to: i) a compressed filament pushes against the membrane; ii) filament and linker pull the membrane while being stretched together; iii) a filament is fully stretched but the linker continues to pull the membrane by being stretched further. Here, $k_\parallel$, k_l and k_{eff} are the linear elastic coefficients of polymer, linker and serial polymer-linker arrangement, respectively. For $k_\parallel$ we use the linear response coefficient of a worm-like chain grafted at both ends [14,15], itself a function of polymer stiffness and contour length [14, pp. 27]. The force F_a affects the detachment rate k_d of attached filaments like

$$k_d(l, \zeta) = k_d^0 e^{-\frac{\delta F_a(l,\zeta)}{k_B T}}. \tag{3}$$

The length of filaments decreases by growth of the actin gel. The gel boundary advances by microscopic processes causing gelation like cross-linking of newly polymerized filaments and entanglement. We call the actin network a gel, when a critical concentration of cross-linkers has been reached. The cross-linking velocity v_g depends on the contour length [29]. It vanishes for $l \to 0$, since cross-linkers cannot bind when $l = 0$. It increases with increasing l, and saturates due to limited cross-linker supply. The velocity v_g can be written as $v_g(l) = v_g^{max} \tanh(l/\bar{l})$ as has been derived from the corresponding reaction-diffusion process in ref. [29]. The characteristic length $\bar{l}$ is inverse proportional to the filament density and the saturation velocity v_g^{max} is proportional to filament density and cross-linker concentration. Here, it is only important that $v_g(l)$ is a saturation function of l. We have chosen $v_g(l) = v_g^{max} l^2/(a + l^2)$ for the purpose of this study to simplify calculations. If filaments are buckled ($l > \zeta$), progression of the gel consumes l/ζ times more contour length of filaments than distance traveled in the lab frame. That causes the factor $\max(1, l/\zeta)$ in the rate of filament shortening $\tilde{v}_g(l, \zeta) = \max(1, l/\zeta) v_g(l)$ [8,11].

The length of filaments increases by polymerization, but only detached, uncapped filaments polymerize. Addition of a monomer to the filament tip requires a sufficiently large gap between the filament tip and the leading edge membrane. The polymerization rate is proportional to the probability for the occurrence of such a gap due to thermal fluctuations [21], which renders it force dependent. Since capping means also the addition of a molecule to the filament tip, the capping rate k_c is also force dependent. We obtain for both rates

$$v_p(l, \zeta) = v_p^{max} e^{-\frac{\delta F_d(l,\zeta)}{k_B T}}, \tag{4}$$

$$k_c(l, \zeta) = k_c^{max} e^{-\frac{d' F_d(l,\zeta)}{k_B T}}. \tag{5}$$

While capping decreases the number of filaments in the semi-flexible region, nucleation generates new filaments. Nucleation generates a Y-shaped, branched structure, since new filaments grow off existing ones. It is different from the simple filaments with respect to the dependence of the force-extension relation on the contour length. The force extension relation of such a structure is not known. Additionally, it would be time dependent since the branching point moves from the membrane into the gel. We circumvent these complications by approximating this force-extension relation by that one of two separate filaments (either F_d or F_a).

2.2 Moment equations

Equations (1a), (1b) for the dynamics of $N_a(l,t)$ and $N_d(l,t)$ can be solved independently from (1c). They have been solved and investigated in several previous publications [8,9,11]. The factor $(\tilde{v}_g - v_p)$ of N_d in the first term on the rhs of Eq. (1a) has a root at l_d. That entails a localization of the distribution at l_d. Therefore we use for $N_d(l,t)$ and $N_a(l,t)$ a mono-disperse approximation and describe them by δ-functions: $N_d(l,t) = n_d(t)\delta(l - l_d(t))$ and $N_a(l,t) = n_a(t)\delta(l - l_a(t))$. Inserting that ansatz into Eqs. (1) and integrating over l we obtain

$$\dot{n}_d(t) = k_d(l_a)n_a(t) - (k_a + k_c(l_d))\, n_d(t) \tag{6}$$

$$\dot{n}_a(t) = k_a n_d(t) - (k_d(l_a) - k_n)\, n_a(t). \tag{7}$$

The moment equation for l_d is obtained by starting from

$$\begin{aligned}
\frac{\partial}{\partial t}\int \mathrm{d}l\; lN_d(l,t) &= \dot{l}_d n_d(t) + l_d k_d(l_a)n_a(t) - (k_a + k_c(l_d))\, l_d n_d(t) \\
\frac{\partial}{\partial t}\int \mathrm{d}l\; lN_d(l,t) &= k_d(l_a)l_a n_a(t) - (k_a + k_c(l_d))l_d n_d(t) \\
&\quad - \int \mathrm{d}l\;\; (\tilde{v}_g(l) - v_p(l))\, n_d(t)\delta(l - l_d) \\
&= k_d(l_a)l_a n_a(t) - (k_a + k_c(l_d))l_d n_d(t) - (\tilde{v}_g(l_d) - v_p(l_d))\, n_d(t).
\end{aligned}$$

Comparing the first and third row leads to

$$\dot{l}_d = -(\tilde{v}_g(l_d) - v_p(l_d)) + k_d(l_a)\frac{n_a(t)}{n_d(t)}(l_a - l_d). \tag{8}$$

Completely analogously we obtain

$$\dot{l}_a = -\tilde{v}_g(l_a) + k_a\frac{n_d(t)}{n_a(t)}(l_d - l_a). \tag{9}$$

Capped polymers will not concentrate at a single length. A detached polymer can not grow any longer and is consumed by the gel after it has been capped. There are capped polymers at all length smaller than l_d. Fortunately, with the δ-ansatz for N_d the equation (1c) can be solved by using the method of characteristics.

$$\frac{\mathrm{d}}{\mathrm{d}t}N_c(l(t),t) = \left(\frac{\partial}{\partial t} - \tilde{v}_g(l)\frac{\partial}{\partial l}\right)N_c(l,t) = N_c(l,t)\frac{\partial}{\partial l}\tilde{v}_g(l) + k_c(l)N_d(l,t), \tag{10}$$

where the characteristics are defined by

$$\frac{\partial l}{\partial t} = -\tilde{v}_g(l). \tag{11}$$

The homogeneous equation (10) is solved by

$$N_c(l(t),t) = C\exp\left(\int_{t_0}^{t}\mathrm{d}t'\;\frac{\partial\tilde{v}_g(l(t'))}{\partial l}\right).$$

Variation of the constant leads to

$$\frac{\mathrm{d}}{\mathrm{d}t}C(t) = k_c(l(t))N_d(l(t),t)\exp\left(-\int_{t_0}^{t}\mathrm{d}t'\,\frac{\partial\tilde{v}_g(l(t'))}{\partial l}\right)$$
$$C(t) = \int_{t_0}^{t}\mathrm{d}t' k_c(l(t'))N_d(l(t'),t')\exp\left(-\int_{t_0}^{t'}\mathrm{d}t''\,\frac{\partial\tilde{v}_g(l(t''))}{\partial l}\right).$$

Therefore the solution for the number distribution of capped polymers is

$$N_c(l(t),t) = \exp\left(\int_{t_0}^{t}\mathrm{d}t'\,\frac{\partial\tilde{v}_g(l(t'))}{\partial l}\right)\int_{t_0}^{t}\mathrm{d}t'\,k_c(l(t'))N_d(l(t'),t')$$
$$\times\exp\left(-\int_{t_0}^{t'}\mathrm{d}t''\,\frac{\partial\tilde{v}_g(l(t''))}{\partial l}\right).$$

Merging the integrals in the exponential functions and using the δ-ansatz for $N_d(l,t)$ we obtain

$$N_c(l(t),t) = \int_{t_0}^{t}\mathrm{d}t'\,k_c(l(t'))n_d(t')\delta\big(l(t')-l_d(t')\big)\exp\left(\int_{t'}^{t}\mathrm{d}t''\,\frac{\partial\tilde{v}_g(l(t''))}{\partial l}\right).$$

We change the integration variable in the exponent with equation (11) to $\mathrm{d}t = -\frac{1}{\tilde{v}_g}\mathrm{d}l$:

$$\exp\left(\int_{t'}^{t}\mathrm{d}t''\,\frac{\partial\tilde{v}_g(l)}{\partial l}\right) = \exp\left(-\int_{l(t')}^{l(t)}\mathrm{d}l'\,\frac{1}{\tilde{v}_g(l')}\frac{\partial\tilde{v}_g(l')}{\partial l'}\right) = \frac{\tilde{v}_g(l(t'))}{\tilde{v}_g(l(t))}.$$

Finally, we reach:

$$N_c(l(t),t) = \sum_{t^*}k_c(l(t^*))n_d(t^*)\frac{1}{|\frac{\mathrm{d}}{\mathrm{d}t}(l(t)-l_d(t))|_{t=t^*}|}\frac{\tilde{v}_g(l(t^*))}{\tilde{v}_g(l(t))}$$
$$= \frac{1}{\tilde{v}_g(l)}\sum_{t^*}\frac{n_d(t^*)k_c(l(t^*))\tilde{v}_g(l(t^*))}{|\frac{\mathrm{d}}{\mathrm{d}t}(l(t)-l_d(t))|_{t=t^*}|}, \tag{12}$$

where t^* is defined by $l(t^*) = l_d(t^*)$. The number of capped polymers of length l is determined by the number of detached polymers and the capping rate at the time the polymers were capped.

t^* can be determined from the characteristic Eq. (11). In the case $\zeta > l_d > l$ we get

$$v_g^{max}\int_{t^*}^{t}\mathrm{d}t' = \int_{l}^{l_d(t^*)}\mathrm{d}l'\,\frac{a+l'^2}{l'^2}$$
$$v_g^{max}(t-t^*) = l_d(t^*) - l + a\,\frac{l_d(t^*)-l}{l_d(t^*)l},$$

and for $l_d > l > \zeta$

$$v_g^{max}\int_{t^*}^{t}\mathrm{d}t'\frac{1}{\zeta(t)} = \int_{l}^{l_d(t^*)}\mathrm{d}l'\,\frac{a+l'^2}{l'^3}$$
$$= \ln\left(\frac{l_d(t^*)}{l}\right) + a\,\frac{l_d^2(t^*)-l^2}{2\,l_d^2(t^*)l^2}.$$

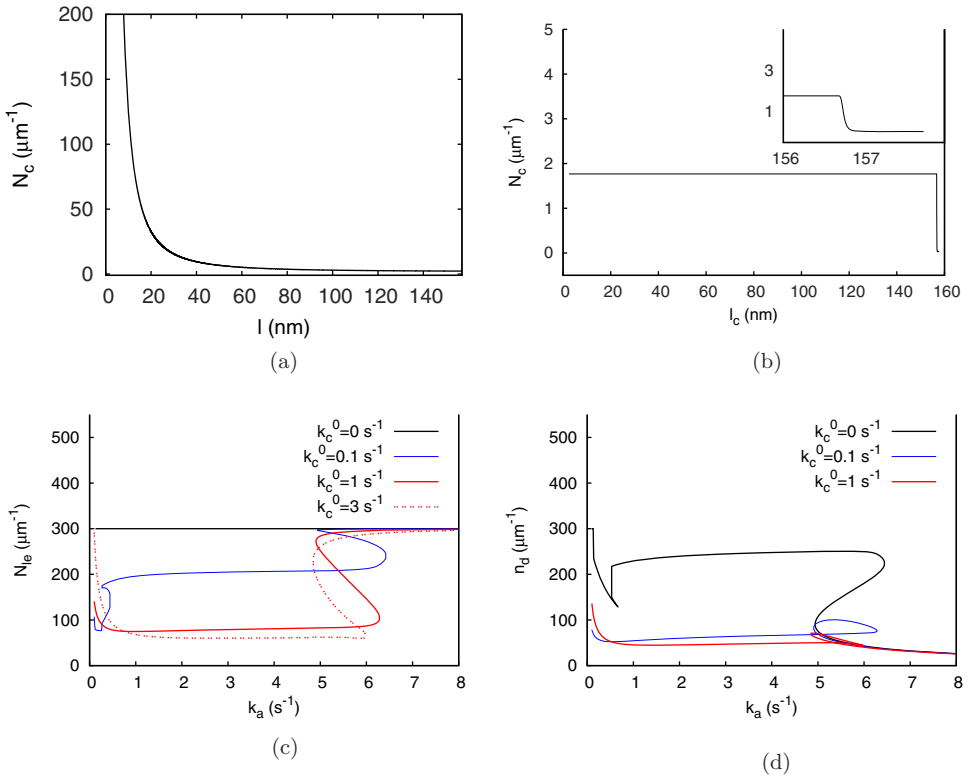

Fig. 2. (a) A typical example for $N_c(l_c)$ in the stationary state with $\tilde{v}_g(l_c,\zeta) = \max(1, l_c/\zeta) v_g^{max} l_c^2/(a+l_c^2)$. The divergence for small l_c is caused by the vanishing cross-linking rate for $l_c \to 0$. (b) The divergence disappears, if we use $\tilde{v}_g(l_c,\zeta) = v_g^{max}$ for $l_c \le \zeta$. The inset shows $N_c(l_c)$ close to the leading edge membrane. It changes only for $l_c > \zeta$. (c) The total number of filaments close to the leading edge membrane N_{le} in dependence on k_a and four values of k_c (v_g^{max}=200 nm s^{-1}). Note the dramatic decrease of filaments caused by capping for $k_a < 5$ s^{-1}. (d) The number of detached filaments for the same k_a-range. Parameter values not mentioned here are in Table 1.

Taking both together for the case $l_d > \zeta > l$ which will be the most important case arising in the actual calculations, we find

$$v_g^{max}\left(t - \tilde{t} + \int_{t^*}^{\tilde{t}} \mathrm{d}t' \frac{1}{\zeta(t)}\right) = \zeta(\tilde{t}) - l + a\,\frac{\zeta(\tilde{t}) - l}{\zeta(\tilde{t}) l} + \ln\left(\frac{l_d(t^*)}{\zeta(\tilde{t})}\right) + a\,\frac{l_d^2(t^*) - \zeta(\tilde{t})^2}{2\,l_d^2(t^*)\zeta(\tilde{t})^2}, \tag{13}$$

where $\tilde{t}$ is defined by $\zeta(\tilde{t}) - l(\tilde{t}) = 0$.

The distribution $N_c(l,t)$ diverges for $l \to 0$ since $\tilde{v}_g(l) \to 0$. Figure 2(a) illustrates that with a typical distribution in the stationary state. This divergence does not occur in the cell since the gel boundary keeps moving even when short capped filaments exist due to the existence of attached and detached filaments (Fig. 2(b)). Filaments which have been capped a long time ago have disappeared from the SR. The 'age' of capped filaments is related to length; old capped filaments are short. Therefore, we take the disappearance of old filaments from the system into account by introducing

Table 1. Parameter values.

Parameter	Value
l_p	$15\,\mu$m
d	2.5 nm
k_l	$1\,\mathrm{pN\,s\,nm^{-1}}$
κ	$10^{-3}\,\mathrm{pN\,s\,nm^{-1}}$
v_p^{max}	$500\,\mathrm{nm\,s^{-1}}$
k_d	$0.5\,\mathrm{s^{-1}}$
k_a	$3\,\mathrm{s^{-1}}$
k_c^0	$1\,\mathrm{s^{-1}}$
v_g^{max}	$300\,\mathrm{nm\,s^{-1}}$
a	$7000\,\mathrm{nm^2}$
k_n^0	$2\,\mathrm{s^{-1}}$
k_n^N	$10^{-3}\,\mathrm{s^{-1}}$

a lower cut off for l in $N_c(l,t)$, which we have chosen to be one monomer length d. Accordingly the total number of filaments is $N_{tot}(t) = n_d(t) + n_a(t) + \int_d^\infty \mathrm{d}l\; N_c(l,t)$.

An equation for the dynamics of the distance between gel boundary and leading edge membrane ζ closes the moment equations. The velocity of the leading edge membrane is determined by the total force balance. Viscous forces, F_a and F_d act on the membrane. The motion of the gel boundary is equal to the average $\tilde{v}_g$ of all three filament populations. That leads to the ζ-dynamics:

$$\dot{\zeta} = \frac{1}{\eta}\Big(F_d(l_d,\zeta)n_d(t) + F_a(l_a,\zeta)n_a(t) + \int_0^\infty \mathrm{d}l\; F_d(l,\zeta)N_c(l,t)\Big) - \frac{1}{N_{tot}}\Big(v_g(l_d)n_d(t) + v_g(l_a)n_a(t) + \int_0^\infty \mathrm{d}l\; v_g(l)N_c(l,t)\Big). \tag{14}$$

3 Results

3.1 Stationary states and the total number of filaments

The system consists now of the dynamics for n_a, n_d, l_a, l_d and ζ. The stationary states are determined by

$$0 = k_d(l_a,\zeta)n_a - k_a n_d - k_c(l_d,\zeta)n_d \tag{15a}$$

$$0 = -k_d(l_a,\zeta)n_a + k_a n_d + k_n n_a \tag{15b}$$

$$0 = v_p(l_d,\zeta) - \tilde{v}_g(l_d,\zeta) + k_d(l_a,\zeta)\frac{n_a}{n_d}(l_a - l_d) \tag{15c}$$

$$0 = -\tilde{v}_g(l_a,\zeta) + k_a\frac{n_d}{n_a}(l_d - l_a) \tag{15d}$$

$$0 = F_d(l_d,\zeta)n_d + F_a(l_a,\zeta)n_a + k_c(l_d,\zeta)n_d \int_\zeta^{l_d} \mathrm{d}l\ \frac{F_d(l,\zeta)}{\tilde{v}_g(l,\zeta)}$$
$$-\frac{\eta}{N}\left(v_g(l_d)n_d + v_g(l_a)n_a + k_c(l_d,\zeta)n_d \int_d^{l_d} \mathrm{d}l\ \frac{v_g(l)}{\tilde{v}_g(l)}\right), \tag{15e}$$
$$\text{where } N = n_d + n_a + k_c(l_d,\zeta)n_d \int_d^{l_d} \mathrm{d}l\ \frac{1}{\tilde{v}_g(l)}.$$

The stationary distribution of capped filaments is related to n_d by Eq. (12) and does therefore not appear explicitly here. The solution of these equations is determined only up to the ratio n_d/n_a. The total number of filaments remains undetermined. Biologically, nucleation is coupled to the total number of filaments via the pool of Arp2/3 molecules. The more filaments exist, the more Arp2/3 is bound and the less is available for nucleation. Therefore, the nucleation rate depends on the total number of filaments $k_n = k_n^0 - k_n^N N$. That fixes the value of N.

The number of filaments close to the leading edge N_{le} determines the force balance and dynamic regime of leading edge motion. It is shown in Fig. 2(c). Interestingly, capping causes a dramatic decrease of N_{le} for small attachment rates. The reason is a strong increase of the number of detached filaments n_d with decreasing attachment rate k_a caused by two saddle-node bifurcations, which occur also without capping (Fig. 2(d)). Filaments become accessible for capping proteins by detachment with this strong rise of n_d, which in the end causes the strong decrease of N_{le}.

Figure 3 shows stationary values in dependence on the maximum capping rate k_c^0 and the filament attachment rate k_a. We observe a dependence of the stationary SR depth ζ and contour lengths l_a and l_d on k_a very similar to the model without capping and nucleation (Fig. 3(a), 3(c), 3(e)). Interestingly, capping may lead either to an increase of the values of these variables or a decrease depending on the value of k_a. Experiments of Bear et al. [2] strongly suggest the case with high values of k_a to apply, where increasing capping leads to shorter filaments. That range of k_a values is also compatible with the theoretical explanation for velocity oscillations of actin-driven lipid vesicles [8] and lamellipodium shape dynamics [9].

3.2 Velocity oscillations

Oscillations of the velocity have been observed with a variety of systems like ActA-coated lipid vesicles [27] and beads [3], with Listeria monocytogenes [10,16], and the leading edge membrane of motile cells [18]. Oscillations have been found with the model with constant numbers of filaments [8,9,11]. We investigate here, whether the system including capping and nucleation also exhibits oscillations.

Examples for oscillations are shown in Fig. 4. The mechanism of oscillation involves periodic attachment and detachment of filaments to the membrane and consists of two phases: A compression phase (e.g. between 12.5 s and 15.0 s in Fig. 4(b)), where the gel boundary advances faster than the membrane. In this phase the fraction of attached filaments is high. Due to the length dependence of forces, both F_d and F_a increase during the compression phase, till the attached filaments can not stand F_d any longer and detach avalanche-like. A relaxation phase follows (e.g. between 15.0 s and 19.0 s in Fig. 4(b)), where the membrane moves faster than the gel and a large fraction of filaments is detached. That phase ends, when forces have decreased to values allowing for re-attachment. This condition initiates a new cycle of protrusion. This mechanism is very similar to the mechanism without capping and nucleation [8,9,11]. As a new phenomenon, we observe a substantial peak of attached filaments due to nucleation just prior to the explosive detachment.

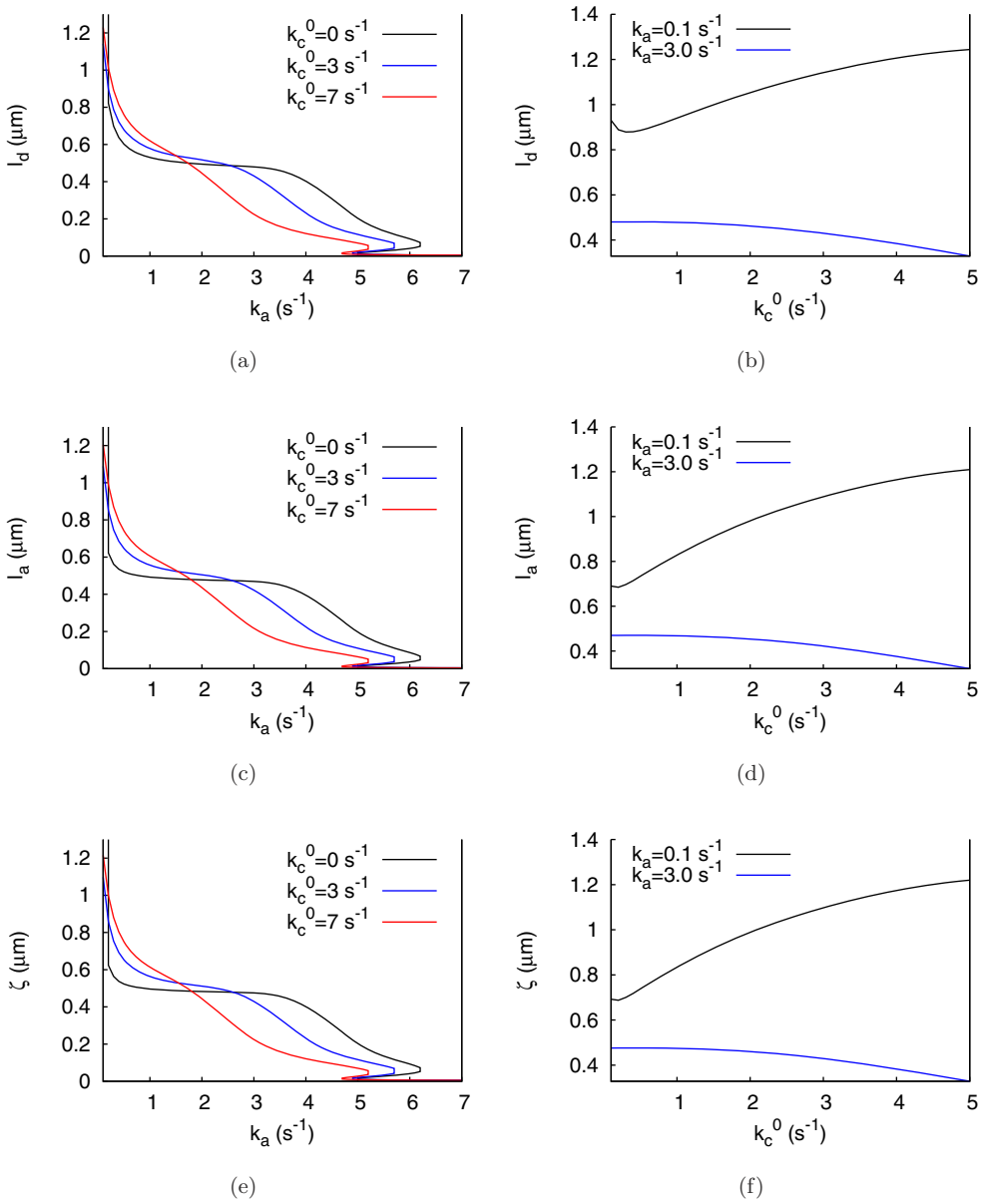

Fig. 3. The stationary filament lengths l_d, l_a and the distance ζ between gel and membrane in dependence on k_a and k_c. Parameter values are in Table 1.

4 Discussion

The main result of this study is a method to include capping and nucleation into a model of the semi-flexible region of the lamellipodial actin network by solving the length distribution dynamics for capped filaments. Development of such a method was required, since capping and nucleation lead to a distribution of capped filaments, which can not be described by the mono-disperse approximation used successfully previously for attached and uncapped detached filaments [8,9,11,21]. Inclusion of

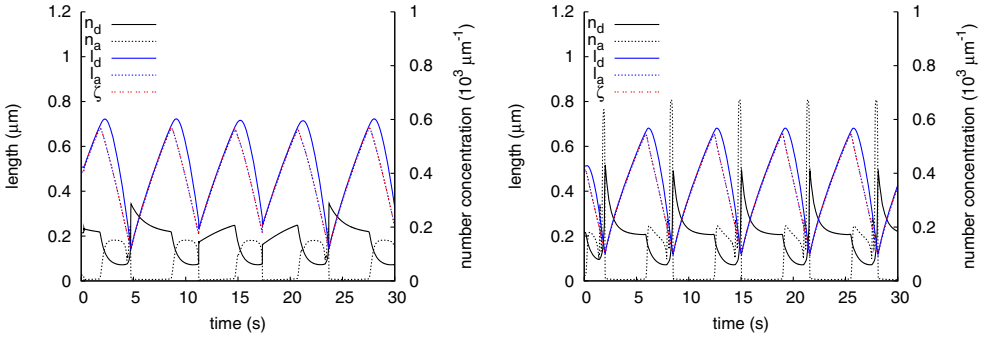

(a) k_c=0.1s^{-1} (b) k_c=0.5s^{-1}

Fig. 4. Oscillations as observed with the parameter values of Table 1, k_a=1.5 s^{-1}.

capping and nucleation did not abolish the variety of dynamic regimes of the semi-flexible region. That is important, since they explain a variety of experimental results with ActA-coated lipid vesicles [8,27] and beads [3,7], with Listeria monocytogenes [10,11,16], and the leading edge membrane of motile cells [9,18].

Capping and nucleation render the number of filaments a dynamic variable. That number may change dramatically even with small capping rates, if the attachment rate is not too large. This effect relies on our assumption that attachment protects filament ends from capping. The sudden change of filament number in dependence on k_a illustrated in Fig. 2 may serve as an experimental test for this hypothesis.

We know the dynamics of the semi-flexible region with capping and nucleation with the complete solution for $N_c(l_c, t)$, now, and can start to think about simplifications to get rid of some of the tedious implications of our approach resulting from the method of characteristics. Our results suggest some possibilities. The cross-linking rate of capped filaments can be replaced by $n_a\tilde{v}_g(l_a) + n_d\tilde{v}_g(l_d) + n_c\tilde{v}_g(l_c)$, since the cross linking rate for capped filaments depends also on the attached and uncapped detached filaments. That will also abolish the divergence of $N_c(l_c, t)$ for $l \to 0$, since l_a and l_d almost never decrease to 0 when retrograde flow is taken into account [29]. Whether we could replace $l^2/(a + l^2)$ even by a constant has to be checked by closer assessment of the cases where l_a and l_d become small. Whatever further simplifications might be done, they should conserve the distribution for $l > \zeta$, since we noticed that these capped filaments contribute substantially to the force balance.

References

1. B. Alberts, D. Bray, J. Lewis, M. Raff, K. Roberts, J.D. Watson, *Molecular Biology of the Cell*, 3rd ed. (Garland Publishing, Inc., New York & London, 1994)
2. J.E. Bear, T.M. Svitkina, M. Krause, D.A. Schafer, J.J. Loureiro, G.A. Strasser, I.V. Maly, O.Y. Chaga, J.A. Cooper, G.G. Borisy, F.B. Gertler, Cell **109**, 509 (2002)
3. A. Bernheim-Groswasser, J. Prost, C. Sykes, Biophys. J. **89**, 1411 (2005)
4. D. Bray, *Cell movements*, 2nd ed. (Garland, New York, 2001)
5. M.F. Carlier, D. Pantaloni, J. Biol. Chem. **282**, 23005 (2007)
6. H.-G. Döbereiner, B.J. Dubin-Thaler, J.M. Hofman, H.S. Xenias, T.N. Sims, G. Giannone, M.L. Dustin, C.H. Wiggins, M.P. Sheetz, Phys. Rev. Lett. **97**, 038102 (2006)
7. M. Enculescu, M. Falcke (submitted)
8. M. Enculescu, A. Gholami, M. Falcke, Phys. Rev. E (Statistical, Nonlinear, and Soft Matter Physics) **78**, 031915 (2008)

9. M. Enculescu, M. Sabouri-Ghomi, G. Danuser, M. Falcke, Biophys. J. **98**, 1571 (2010)
10. F. Gerbal, P. Chaikin, Y. Rabin, J. Prost, Biophys. J. **79**, 2259 (2000)
11. A. Gholami, M. Falcke, E. Frey, New J. Phys. **10**, 033022 (2008)
12. A. Gholami, J. Wilhelm, E. Frey, Phys. Rev. E **74**, 041803 (2006)
13. E. Gouin, M.D. Welch, P. Cossart, Curr. Opinion Microbiol. **8**, 35 (2005)
14. K. Kroy, *Viskoelastizität von lösungen halbsteifer polymere* (Hieronymus, München, 1998)
15. K. Kroy, E. Frey, Phys. Rev. Lett. **77**, 306 (1996)
16. I. Lasa, E. Gouin, M. Goethals, K. Vancompernolle1, V. David, J. Vandekerckhove1, P. Cossart, EMBO J. **16**, 1531 (1997)
17. T.P. Loisel, R. Boujemaa, D. Pantaloni, M.-F. Carlier, Nature **401**, 613 (1999)
18. M. Machacek, G. Danuser, Biophys. J. **90**, 1439 (2006)
19. Y. Marcy, J. Prost, M.-F. Carlier, C. Sykes, Proc. National Acad. Sci. United States Amer. **101**, 5992 (2004)
20. A. Mogilner, G. Oster, Biophys. J. **71**, 3030 (1996)
21. A. Mogilner, G. Oster, Biophys. J. **84**, 1591 (2003)
22. S.H. Parekh, O. Chaudhuri, J.A. Theriot, D.A. Fletcher, Nat. Cell Biol. **7**, 1219 (2005)
23. J. Plastino, C. Sykes, Curr. Opinion Cell Biol. **17**, 62 (2005)
24. T.D. Pollard, G.G. Borisy, Cell **112**, 453 (2003)
25. A. Ponti, M. Machacek, S.L. Gupton, C.M. Waterman-Storer, G. Danuser, Science **305**, 1782 (2004)
26. T.M. Svitkina, A.B. Verkhovsky, K.M. McQuade, G.G. Borisy, J. Cell Biology **139**, 397 (1997)
27. L. Trichet, O. Campàs, C. Sykes, J. Plastino, Biophys. J. **92**, 1081 (2007)
28. P. Vallotton, G. Danuser, S. Bohnet, J.-J. Meister, A.B. Verkhovsky, Mol. Biol. Cell **16**, 1223 (2005)
29. J. Zimmermann, M. Enculescu, M. Falcke, Phys. Rev. E **82**, 051925 (2010)
30. A. Zumdieck, M.C. Lagomarsino, C. Tanase, K. Kruse, B. Mulder, M. Dogterom, F. Jülicher, Phys. Rev. Lett. **95**, 258103 (2005)